Deep Percolation and Gas Transport in a Soil Cover

GEO-SLOPE International Ltd. | www.geo-slope.com

1200, 700 - 6th Ave SW, Calgary, AB, Canada T2P 0T8
Main: +1 403 269 2002 | Fax: +1 888 463 2239

Introduction

This example illustrates how to simulate the performance of an engineered soil cover system in response to land-climate interaction. The primary objective of the simulation is to assess deep percolation and oxygen ingress through the base of the cover into the waste. A commentary on various aspects of land-climate interaction modeling is discussed, with a particular emphasis on interpreting the results and closing the water balance for the cover.

Numerical Simulation

Figure 1 shows the model domain and Figure 2 shows the details of the surface mesh. The Surface Layers are drawn on top of a conventional region.

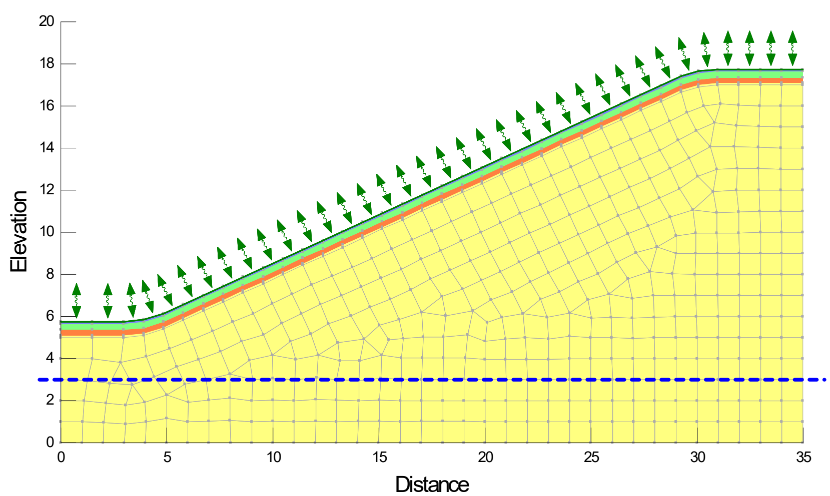

Figure 1. Model domain for the simulated soil cover over waste.

The use of Surface Layers, in combination with a structured and dense mesh, is numerically advantageous in cases where large spatial variations in pore-water pressure might exist. In this case, the cover is designed to promote a capillary break at the base of low conductivity materials (i.e. the orange material). As such, large spatial variations in pore-water pressure are expected to exist at the base of the cover.

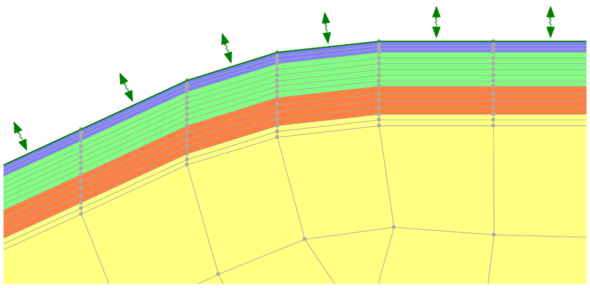

Figure 2. Detail of the surface mesh.

Three physical processes are being solved on the domain: water transfer, heat transfer, and gas transfer (Figure 3). The water transfer analysis includes isothermal and thermally-driven vapor flow, which can be important when evaporative drying is involved. The heat transfer analysis includes forced-convection via liquid water and vapor transfer in addition to the default conduction-only process. Only the default physics for gas transfer is selected, which implies a diffusion-only system.

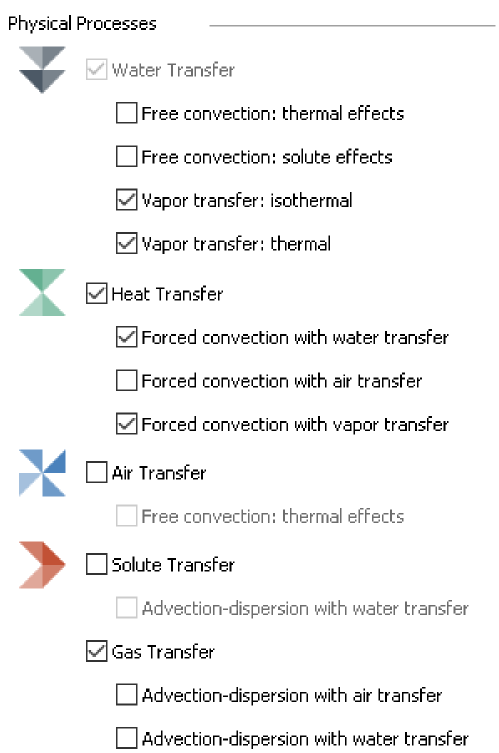

Figure 3. Physics selection for analysis.

The cover comprises three materials. The orange layer represents a low conductivity compacted clay layer that is designed to remain near saturation, which in-turn limits oxygen diffusion thereby preventing various chemical reactions within the waste. Two growth layers exist above the compacted unit (green and purple).

There are a number of attributes of the problem definition that should be explored in the GeoStudio file including:

- The initial pore-water pressure conditions are obtained from a water table. The pore-water pressures vary hydrostatically below and above the water table, but are truncated above the water table at the specified maximum negative pressure head.
- The initial pore-water pressures in the cover layers are established using the activation value in the material models. This over-rides the value from the water table for these materials.
- The initial temperatures for all layers are obtained using the activation values in the material models.
- The diffusion of oxygen is being simulated and the initial gas concentrations are specified by activation in the material models.
- The water transfer analysis includes the effect of ground freezing on the hydraulic conductivity. This option is selected in the material model.
- The simulation includes vegetation. Nodes within the specified root zone, as defined by the root depth function, will uptake water if the soil suctions are not above the wilting pressure.

Material properties

Figure 4 shows the volumetric water content functions for the three soils: waste, a compacted low permeability layer, and a growth layer. The waste layer has the lower porosity and the compacted clay layer the highest. The volumetric water content function characterizes the capacity of a soil to store or release water as a result of changes in pore-water pressure. As such, these functions can have a significant effect on the performance of a soil cover subject to cycles of wetting and drying.

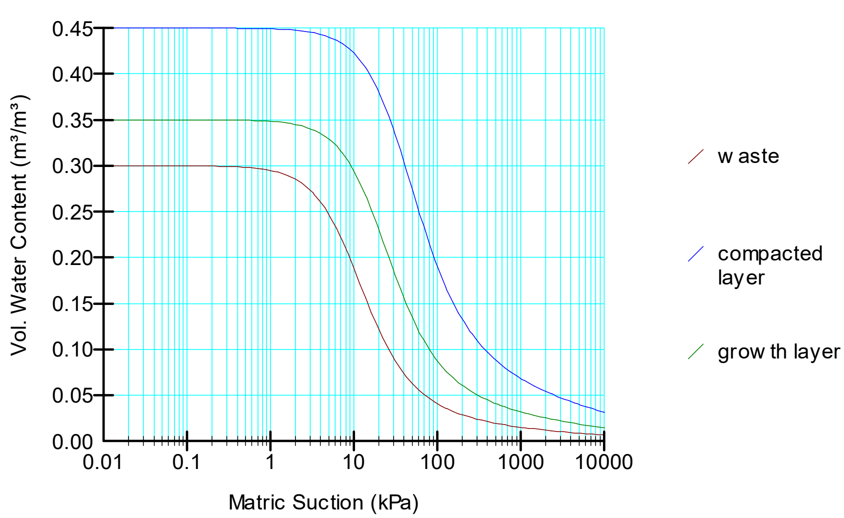

Figure 4. Water content functions.

Figure 5 presents the hydraulic conductivity functions. The hydraulic conductivity functions can be defined from measured data or estimated from the volumetric water content functions according to the methods of van Genuchten or Fredlund and Xing. An add-in function can also be used. In this case, the van Genuchten estimation technique was used. The upper part of the growth layer has a modified function that is truncated at a higher conductivity at large suctions (i.e. when the soil is dry). This modification to the function attempts to account for desiccation (cracking), root penetration, and alteration by other surface processes.

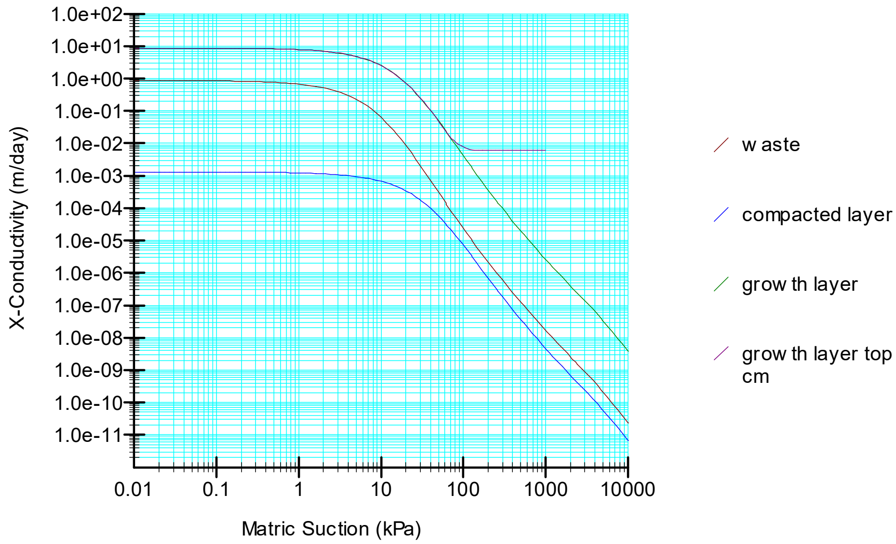

Figure 5. Hydraulic conductivity functions.

The Simplified Thermal model was used to represent all of the materials, which requires specification of the frozen and unfrozen thermal conductivity and volumetric heat capacity (Figure 6). The assumptions associated with the simplified model are: a) thermal conductivity does not vary with volumetric water content; and, b) all water within the pore-space changes phase instantly instead of over a temperature range. The Simplified Thermal model is generally adequate if the thermal response during freeze/thaw is not the primary interest. Figure 6 also shows the activation temperature of the material.

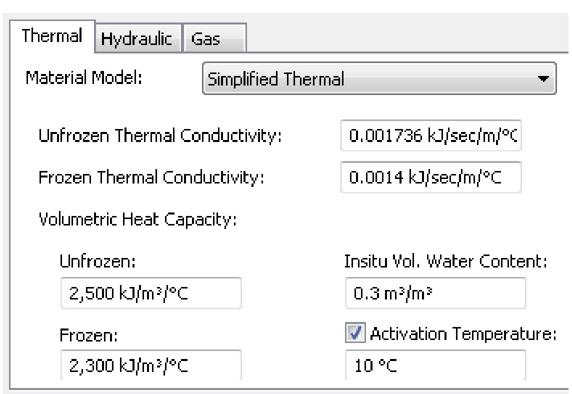

Figure 6. Thermal properties.

The gas properties are shown in Figure 7. The CTRAN/W gas transfer formulation gives consideration to dispersion and advection in both the gas and dissolved phases. For this example, transport in the dissolved phase is ignored and dispersion in the gas phase is considered negligible. An input for the dispersivity coefficient is not visible on the gas material tab because advection-dispersion with air transfer was not selected as a physics option (Figure 3). The bulk diffusion coefficient ($D^*_{d(a)}$) of oxygen was estimated according to Aachib et al. (2004) as:

$$D^*_{d(a)}\theta_a = \frac{1}{n^2}\left(D^0_a \theta_a{}^x\right)$$ Equation 1

where the exponents are evaluated as:

$$x = 1.201\theta_a^3 - 1.515\theta_a^2 + 0.987\theta_a + 3.119$$ Equation 2

and the exponent y is evaluated as:

$$y = 1.201\theta_w^3 - 1.515\theta_w^2 + 0.987\theta_w + 3.119$$ Equation 3

The free phase diffusion coefficient for oxygen in air is $D^0_a \cong 1.8E-5$ m²/s and the air content (θ_a) is calculated as the difference between the porosity (n) and water content.

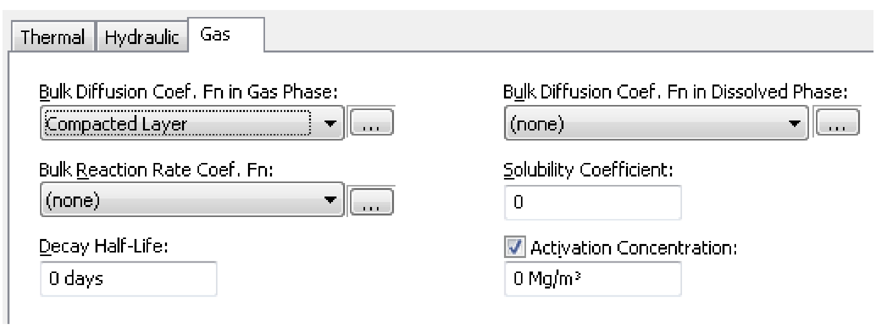

Figure 7. Gas transfer material properties.

Boundary Conditions

The following boundary conditions are applied to the domain:

1. Total head of 3 m along the left vertical edge;
2. Constant temperature of 10°C along the base of the domain;
3. Land-climate interaction mass (i.e. water) along the ground surface;
4. Temperature vs time function along the ground surface; and,
5. Oxygen gas concentration of 2.80e-4 Mg/m³ along the ground surface.

The ground temperature is assumed equal to the air temperature, which is an approximation of a surface energy balance. There are two alternatives in GeoStudio that could have been used: 1) the n-factor approach, which requires an air temperature vs. time function with a modifier; or, 2) the land-climate interaction energy boundary condition. The latter performs an actual surface energy balance. The lower temperature boundary is arbitrary and only for demonstration purposes. Ultimately, a geothermal heat flux should be used if the thermal results are of interest, with the lower boundary moved further away from the active zone.

The land-climate interaction mass boundary calculates the net infiltration flux at the ground surface and/or root water uptake from within the domain. A climate data set and vegetation data set must be associated with the boundary condition (Figure 8). The Penman-Wilson method is used in this example to calculate the actual evapotranspiration flux. The method can also be used to calculate the potential evapotranspiration, which, when combined with information about the vegetation, can be used to calculate the root water uptake (see other examples and Engineering Book for more information). Precipitation and snowmelt flux are determined from the corresponding climate data functions.

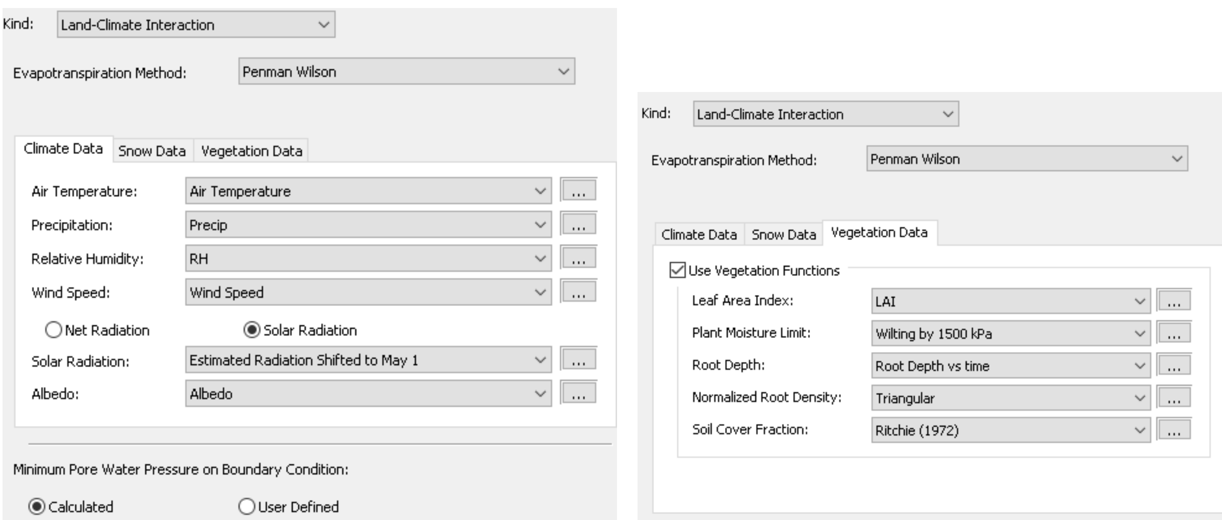

Figure 8. Inputs for the land-climate interaction mass boundary condition.

The minimum pore-water pressure toggle in Figure 8 ensures that soil does over-dry across a time step, causing the soil and atmosphere to be in disequilibrium. There are two options: 1) a user-input pore-water pressure vs time function; and, 2) an internally calculated value. The latter approach calculates the minimum pore-water pressure as:

$$\varphi = ln(RH)\rho_w RT/\omega_v$$ **Equation 4**

where RH is relative humidity, ρ_w is the density of water, R is the universal gas constant, T is temperature, and ω_v is molecular weight of water vapor.

All of the functions used to define the climate and vegetation should be reviewed. The leaf-area index reaches a value of 2.0 at the peak of the growth season. The soil cover fraction, which controls the partitioning of potential evapotranspiration to actual evaporation and root water uptake, was calculated using the equation proposed by Ritchie (1972):

$$SCF = 1 - e^{-k(LAI)}$$ Equation 5

where LAI is the leaf area index and k is a constant governing the radiation extinction by the canopy as a function of sun angle, the distribution of plants, and the arrangement of leaves (varies between 0.5 and 0.75). The SCF was calculated assuming a value of 0.75.

The normalized water uptake distribution $\pi_{root}^{'}$ (L^{-1}) is given as:

$$\pi_{root}^{'} = \frac{\pi_{root}}{\int_0^{r_{max}} \pi_{root} dr}$$ Equation 5

where π_{root} is the root length density (L/L^3); that is, the length of root per volume of soil. The normalized root density function was assumed to be triangular and calculated according to Prasad (1988) assuming a maximum root depth of 0.4 m (Figure 9):

$$\pi_{root}^{'} = \frac{2}{r_{max}}\left(1 - \frac{r}{r_{max}}\right) \quad r \leq r_{max}$$ Equation 6

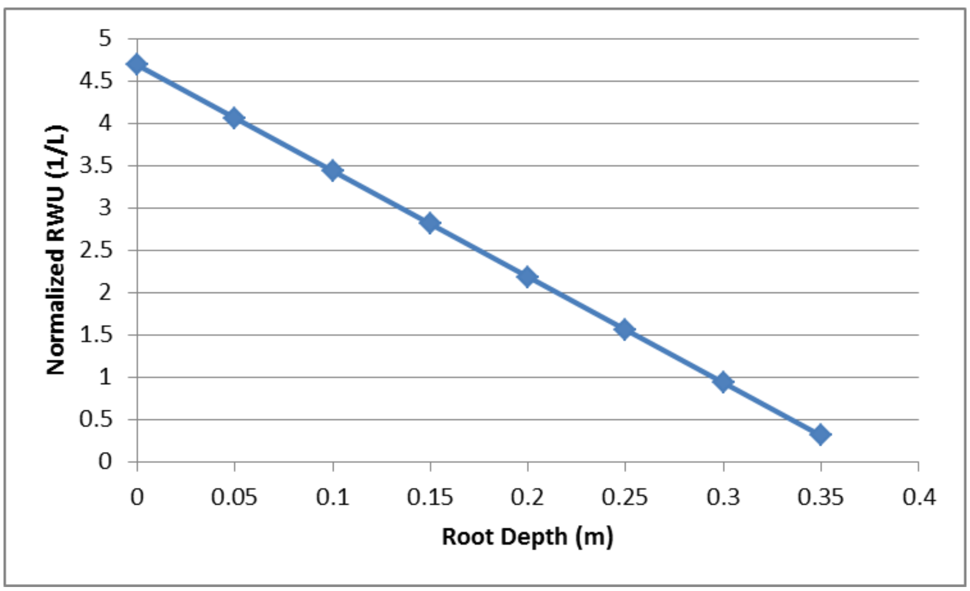

Figure 9. Normalized root water uptake verses root depth.

The relationship shown in Figure 9 is limiting because the root depth cannot change with time. As such, the SEEP/W mass LCI utilizes a normalized root density versus normalized root depth function:

$$\frac{\pi_{root}}{\pi_{root}^{max}} \, vs \, \frac{r}{r_{max}}$$ Equation 7

where the root length density π_{root} at every depth is normalized by the maximum value in the profile π^{max}_{root} and defined versus the normalized depth. Normalization of the triangular (normalized) root water uptake function produces the result shown in Figure 10. SEEP/W performs the integration of the function and other required calculations to obtain the normalized water uptake π'_{root} at any particular depth.

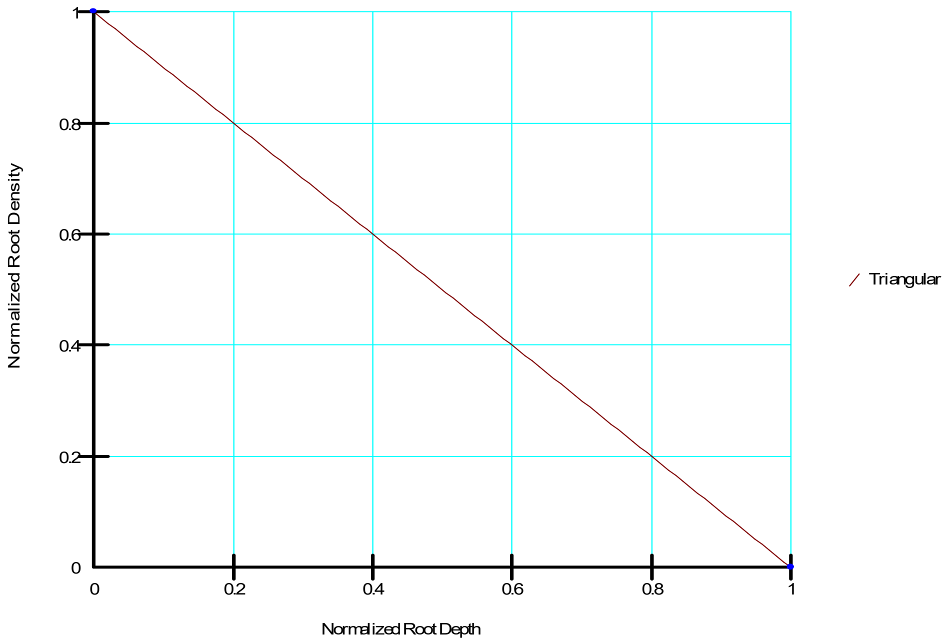

Figure 10. Normalized root density versus normalized root depth.

Time Definition

The duration of the analysis is set to 200 days using 2400 time steps. As such, each time step has an elapsed time of 2 hours. Every 12th time step (1 day) is saved.

Results and Discussion

Surface Water Balance

The following equation must be satisfied in order to close the water balance:

$$(q_P + q_M)cos\alpha + q_E + q_R = q_I \quad \text{Equation 1}$$

where superscripts on the water fluxes (q) indicate rainfall (P), snow melt (M), infiltration (I), evaporation (E) and runoff (R) and α is the slope angle. The evaporation and runoff fluxes are negative; that is, out of the domain. Transpiration is not typically included in the surface water balance; however, it must be included for this example because the root distribution extends to the ground surface. As such, the net infiltration reported by SEEP/W includes root water uptake reported to the ground surface nodes.

Figure 11 plots of the surface water balance components in cumulative volume including net infiltration, rainfall, evaporation, runoff, and transpiration at the ground surface. The water balance can be interpreted as follows:

a. There was 0.0 m^3 or runoff (not shown)

b. The total rainfall was 0.682 m^3;

c. Evaporation removed -0.999 m^3 and transpiration at the ground surface removed -0.222m^3;

d. The net infiltration at the end of the analysis was -0.54m^3; and,

e. The water balance is zero (i.e. closed) for the entire anlaysis.

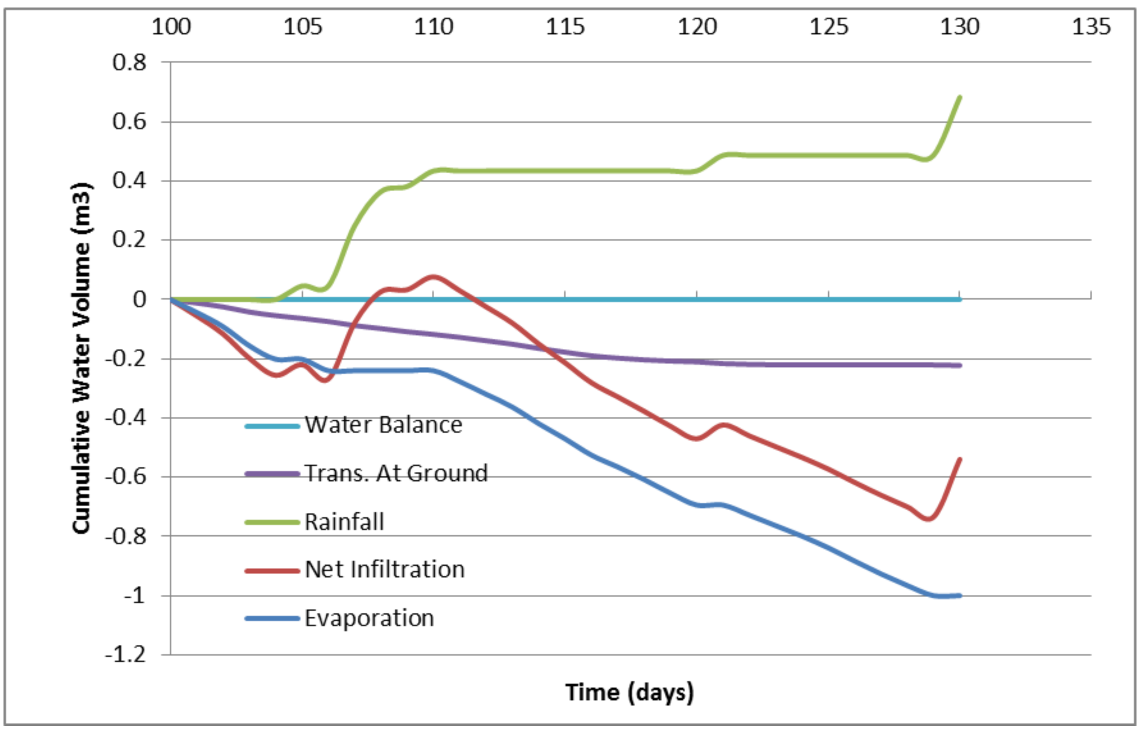

Figure 11. Surface water balance.

Deep Percolation

Figure 12 shows the cumulative volume of water versus time moving past the base of the cover (i.e. interface between compacted layer and waste) and at the base of the root zone (i.e. interface between growth layer and compacted layer). These plots are generated using nodal data of a sub-domain graph. A sub-domain graph is required because a conventional graph will report zero flow rates and cumulative volumes at all nodes without a specified boundary condition. A positive value indicates flow into the sub-domain, while a negative indicates flow out of the sub-domain. A total of -0.063 m^3 reported as deep percolation into the waste rock – that is, past the base of the compacted layer – by the end of the analysis. In contrast, 1.37 m^3 of water moved upwards past the base of the root zone to meet the demands of the roots. In actuality, the net cumulative water volume might have been negative at the base of the compacted layer by the end of the analysis; however, water flow was upwards through the base of the compacted layer beginning at around Day 107 because of the root water uptake.

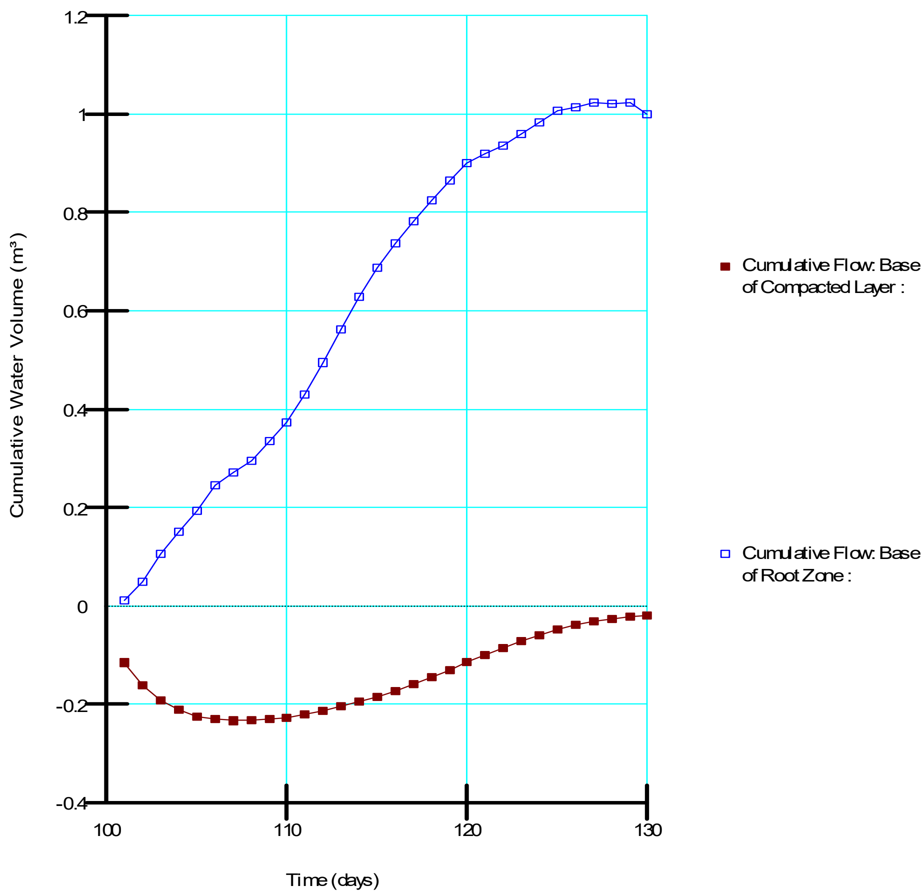

Figure 12. Time history of the cumulative flow volume of water (liquid and vapor) at the base of the root zone layer and compacted layer.

It should also be noted that root water uptake throughout most of the root zone ceases at around Day 120. This is evident in the water balance graph for cumulative transpiration (Figure 13). An inspection of the pore-water pressure in the GeoStudio file reveals that the pore-water pressures exceed in the wilting throughout most of the root zone.

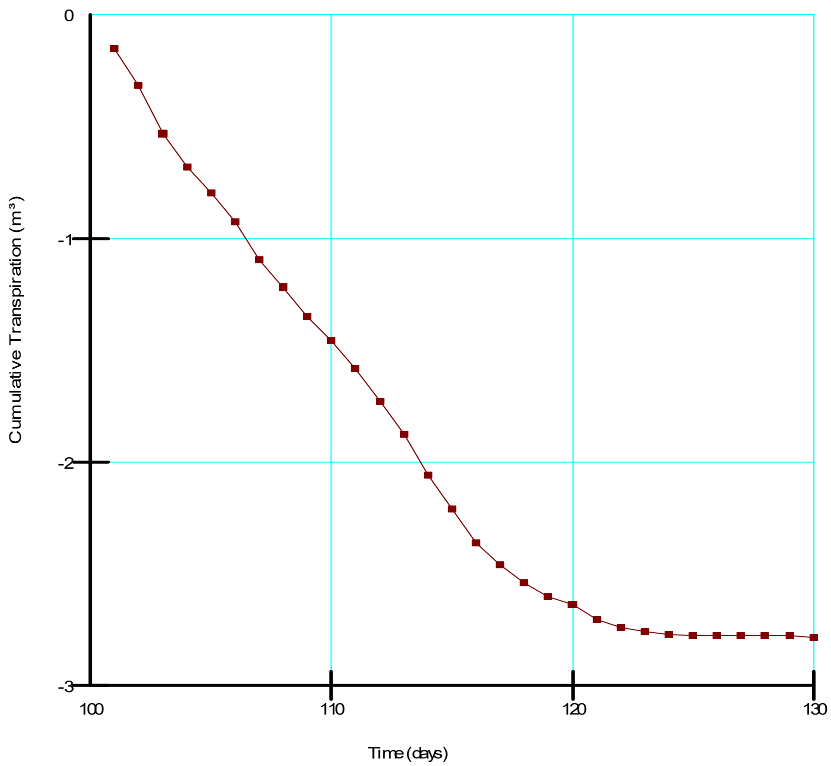

Figure 13. Cumulative transpiration from the root zone.

Figure 13 shows the water rate at each individual node plotted versus x-coordinate at the base of the compacted layer on Day 101 and Day 130. This graph is again created using a sub-domain. The result indicates that:

1. At the onset of the analysis, there was a net downwards (negative) movement of water out of the base of the compacted layer from about x = 6 m to the right edge of the domain.
2. On Day 130, water flow is upwards into the compacted layer from the left edge of the domain to the crest. There is some deeper percolation occurring at the top of the hillslope. There was a significant rainfall event on Day 130, however, the over-all upwards flow is a reflection of the greater availability of water for root uptake at lower elevations.

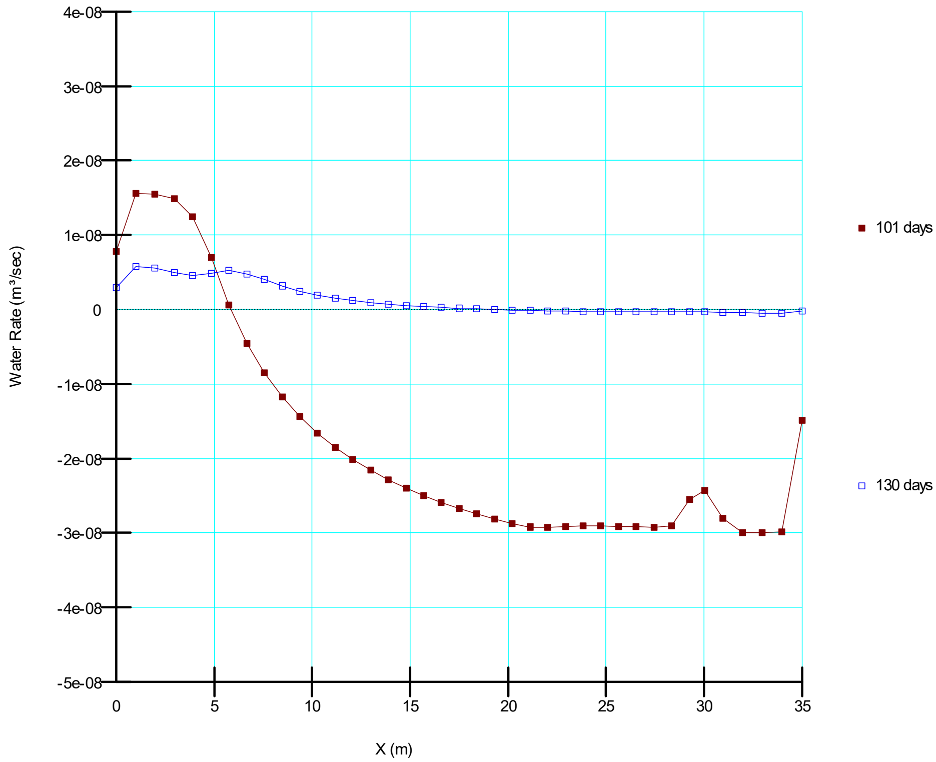

Figure 14. Water rates at nodes located at the base of the compacted layer on Day 101 and Day 130.

In summary, the entire compacted layer – from the left to the right of the domain – is in a drier state by the end of the analysis due mostly to root water uptake, although deep percolation at the onset of the analysis also contributed to a loss of water from the cover system.

Water Content and Gas Transfer

Figure 14 and Figure 15 show the volumetric water content profiles along the left and right edges of the model. The compacted layer extends from elevation 5.1 to 5.35 m and 17.1 m to 17.35 m on the left and right edges of the domain, respectively. The compacted layer maintains near saturation conditions near the toe of the slope (left edge), while approaching a water content of 0.2 further upslope. The growth layer is nearing the residual water content due primarily to transpiration. The effects of retaining water through part of the compacted layer are reflected in profiles of gas concentration (Figure 16 and Figure 17). The gradient in O^2 concentration across the compacted layer is greater throughout the analysis near the toe due to the higher degree of saturation and lower coefficient of diffusion. Regardless, the desaturation of most of the cover results in fairly rapid O^2 ingress.

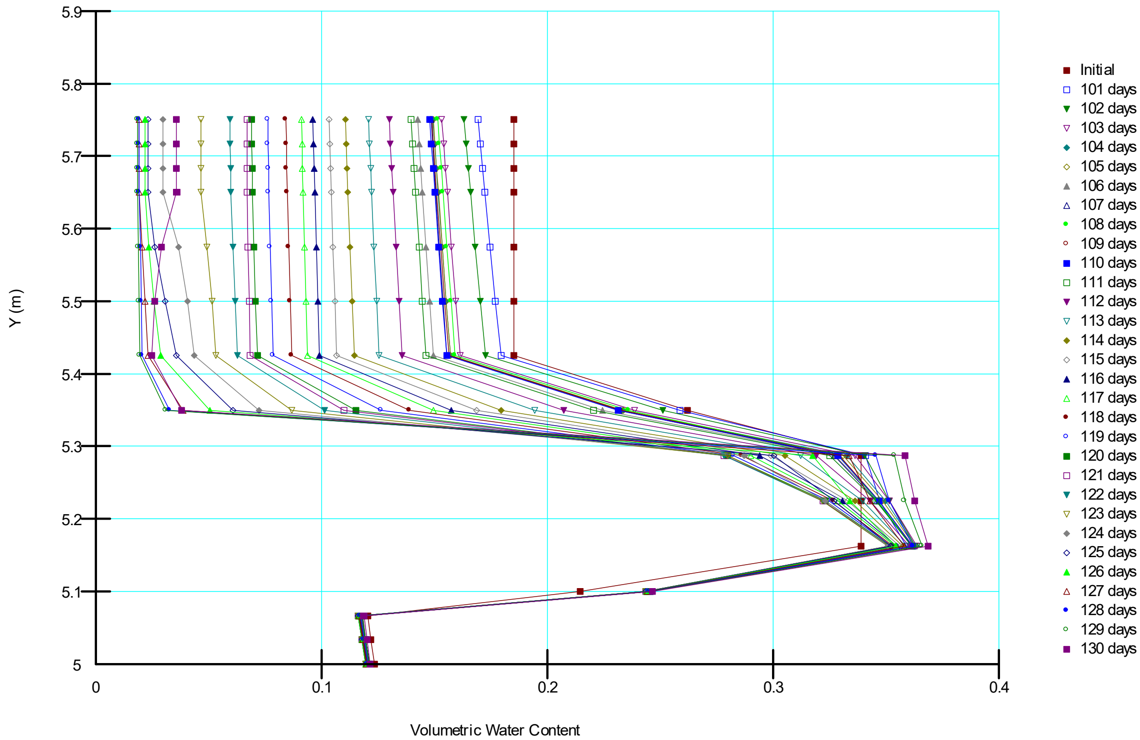

Figure 15. Volumetric water content profile through the cover along the left edge of the model

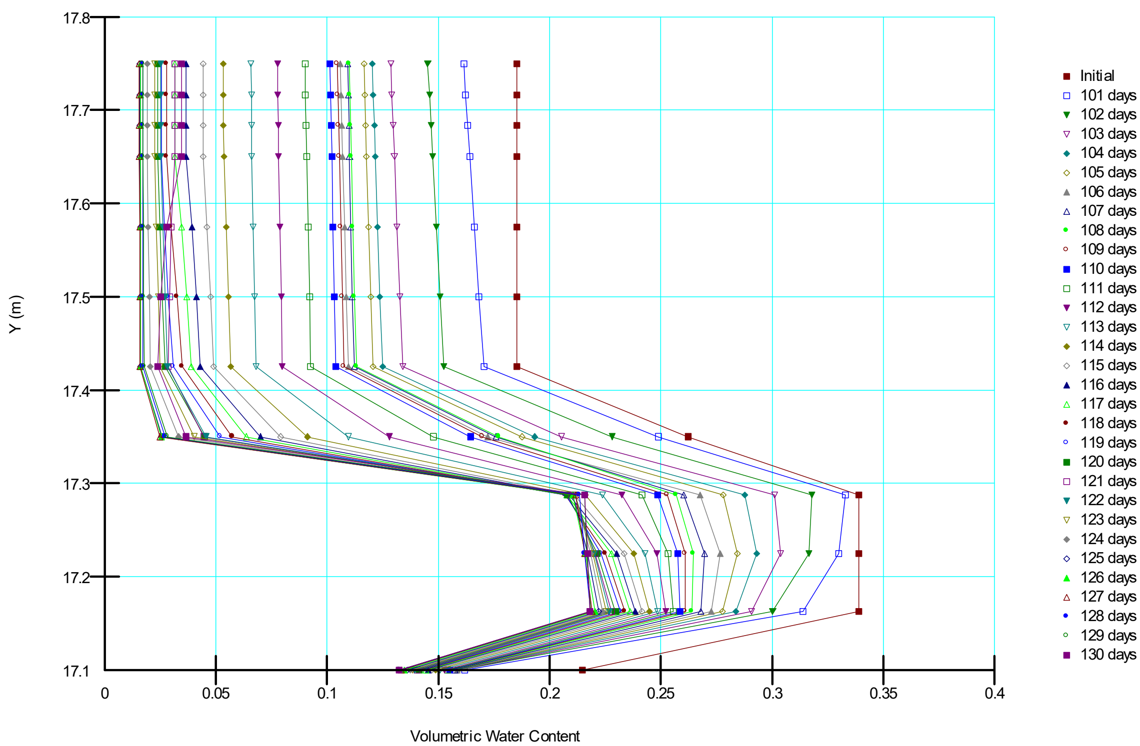

Figure 16. Volumetric water content profile through the cover along the right edge of the model

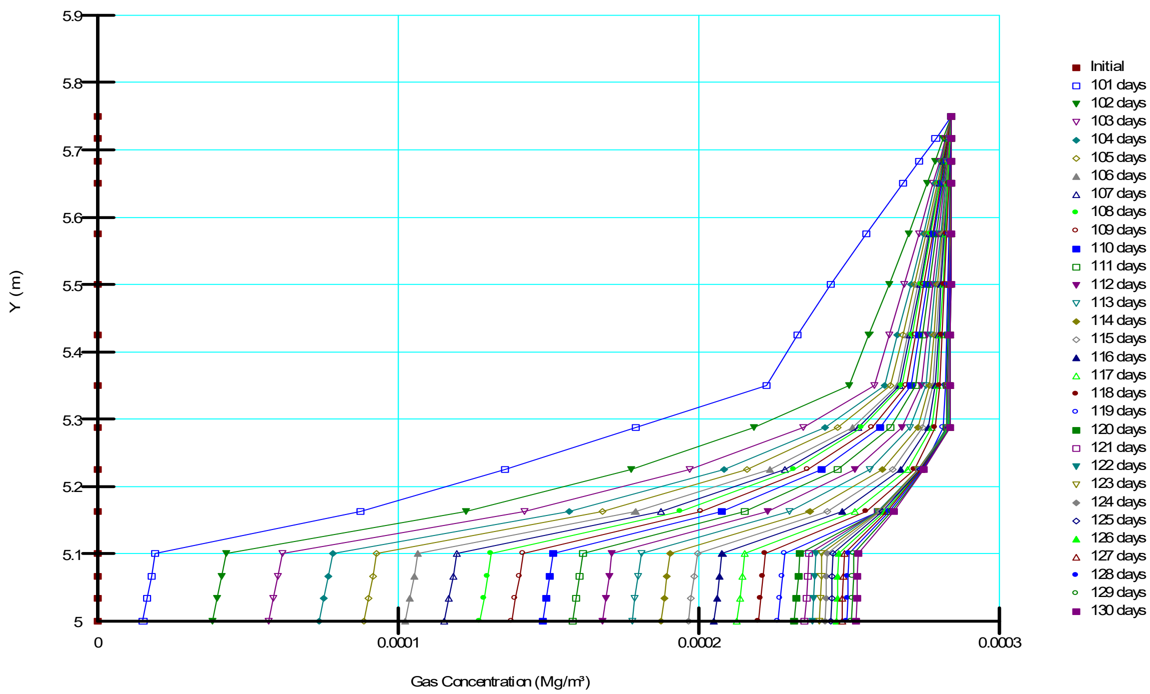

Figure 17. Gas concentration profile through the cover along the left edge of the domain.

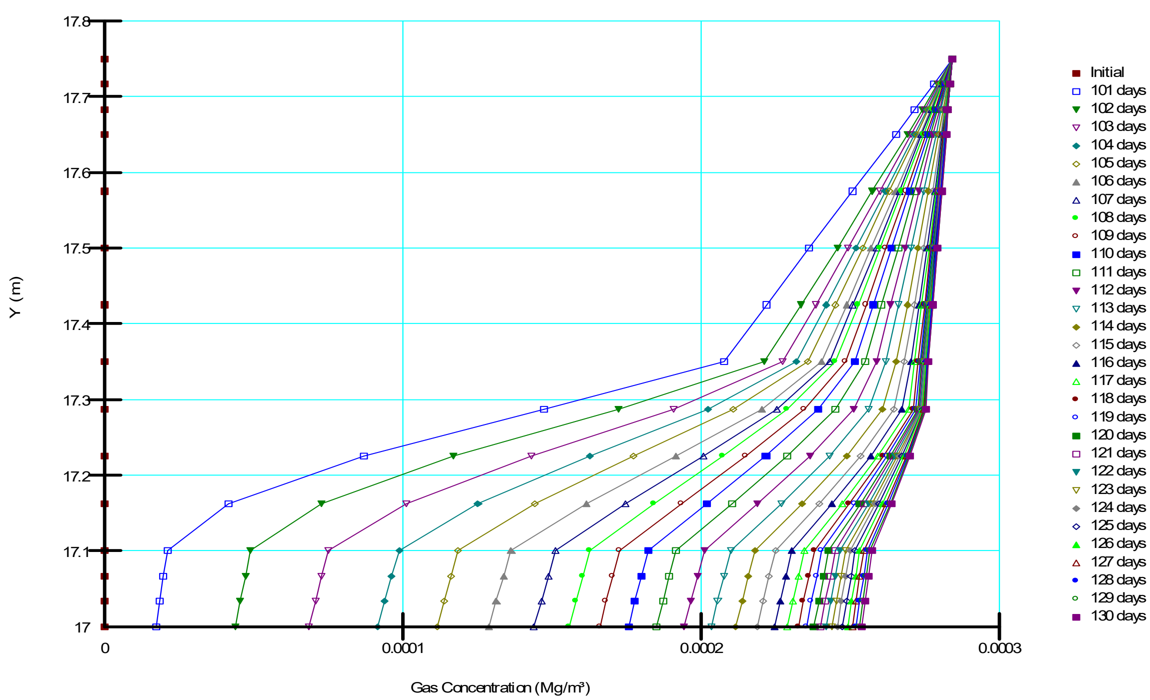

Figure 18. Gas concentration profile through the cover along the right edge of the domain.

Mass Balance Error

Non-convergence at any time step of a transient finite element analysis can manifest in an inequality between the rate of change in the mass of water stored within the domain and the rate at which water enters and leaves the domain. The difference between the cumulative change in mass of water within the domain and the cumulative mass that leaves or enters the domain provides a measure of the error. A relative error could be calculated by dividing the absolute error by the maximum of the two values. The mass balance error and its components can be plotted for the entire domain or portion of the domain; that is, a sub-domain. Figure 19 was generated for the entire domain (refer to the associated file). The cumulative change in mass within the domain is generally commensurate with the cumulative change at the boundaries, including root water uptake. The mass balance error is therefore negligible.

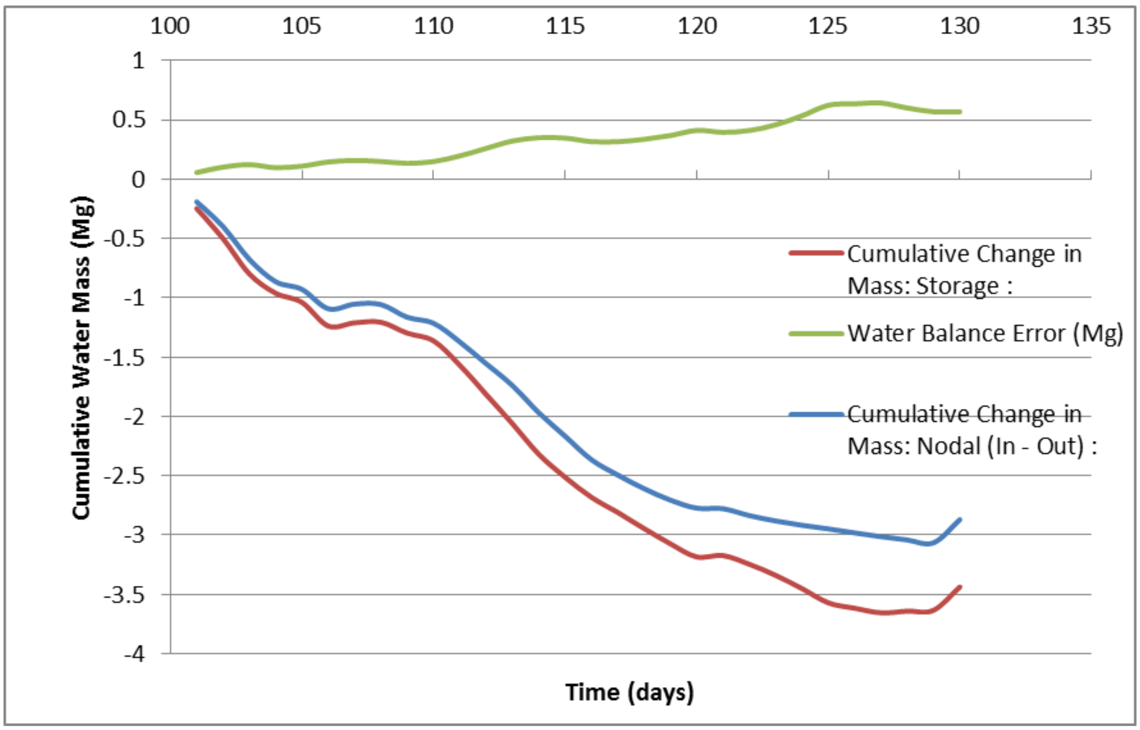

Figure 19. Mass balance check for the entire domain.

Summary and Conclusion

The interpretation of soil cover systems is a rather involved process. The preceding discussion demonstrated only a fraction of the number of graphs that can be generated to assist with interpretation. In order to interpret the results of a soil cover analysis it is important to give consideration to water flow between the various layers, inspect material parameters such as water content, and most importantly, to close the water balance. Closing the water balance implies that all surface recharge/discharge, root-water uptake, and boundary flows are reflected in the change in storage. A water balance can be calculated for the entire domain or for the cover layer alone.